Author

Tie Sun

Title

Excess air in the noble gas groundwater paleothermometer: A new model based on diffusion in gas phase.

Submitted for Publication in:

Geophysical Research. Letters

in lieu of thesis in partial fulfillment
of the requirements for the degree of
Master of Science in Geology
Department of Geological Sciences
The University of Michigan

Accepted by:

Signature	MARIA CLARA CRUZ DA SILVA CASTRO	2/12/08
	Name	Date
Signature	CHRIS HALL	12/2/08
	Name	Date
Department Chair	SAMUEL B MUKASA	12/3/08
	Name	Date

I hereby grant the University of Michigan, its heirs and assigns, the non-exclusive right to reproduce and distribute single copies of my thesis, in whole or in part, in any format. I represent and warrant to the University of Michigan that the thesis is an original work, does not infringe or violate any rights of others, and that I make these grants as the sole owner of the rights to my thesis. I understand that I will not receive royalties for any reproduction of this thesis.

☒ Permission granted.

☐ Permission granted to copy after: _____
Date

☐ Permission declined.

Tie Sun
Author Signature

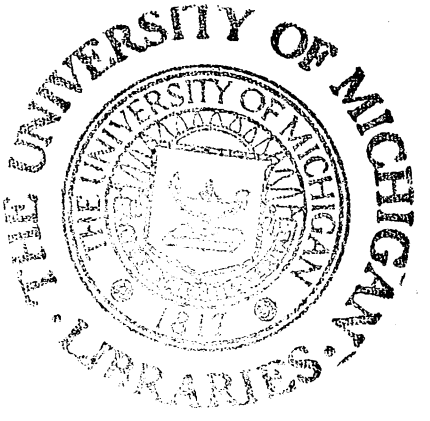
THE UNIVERSITY OF MICHIGAN
LIBRARIES

GEOPHYSICAL RESEARCH LETTERS, VOL. 35, L19401, doi:10.1029/2008GL035018, 2008

Excess air in the noble gas groundwater paleothermometer: A new model based on diffusion in the gas phase

Tie Sun,[1] Chris M. Hall,[1] Maria Clara Castro,[1] Kyger C. Lohmann,[1] and Patrick Goblet[2]

Received 13 June 2008; accepted 22 August 2008; published 4 October 2008.

[1] A key assumption for calculating paleotemperatures using noble gas concentrations in groundwater is that water equilibrates with standard air. However, if the unsaturated zone is depleted in O_2, the noble gas partial pressures will be elevated, resulting in a bias of noble gas temperatures (NGTs) to low values. This oxygen depletion (OD) mechanism was used to explain low NGT values for a shallow aquifer in Michigan where new O_2 saturation and CO_2 measurements now confirm the OD model. Measured excess He, without an expected vertical concentration gradient in the water phase, suggests that the rate of noble gas equilibration at the base of the unsaturated zone is restricted, and that transport within the gas phase may be a rate-limiting step. A new NGT model is presented that uses the OD mechanism and that allows for partial re-equilibration of excess air via diffusion in the gas phase.
Citation: Sun, T., C. M. Hall, M. C. Castro, K. C. Lohmann, and P. Goblet (2008), Excess air in the noble gas groundwater paleothermometer: A new model based on diffusion in the gas phase, *Geophys. Res. Lett.*, *35*, L19401, doi:10.1029/2008GL035018.

1. Introduction

[2] Noble gas temperatures (NGTs), which are derived from the air saturated water (ASW) component of noble gas concentrations (Ne, Ar, Kr, Xe) in groundwater have long held out the promise of providing a robust absolute thermometer for use in paleoclimate reconstructions [*Stute and Schlosser*, 1993]. In principle, groundwater noble gas concentrations are a simple function of the temperature at the water table at the time of recharge, with only a small set of assumptions needed. These assumptions include a) solubility equilibrium between noble gases and water; b) noble gas partial pressures as determined by standard atmospheric values for the altitude of recharge; c) 100% relative humidity at the air-water interface; and d) temperature dependent noble gas solubilities determined by ground temperature at the time of recharge. Early on it was found that in addition to a temperature dependent ASW component, groundwater also incorporates an extra "excess air" component [*Heaton and Vogel*, 1981] caused by the partial or total incorporation of disconnected air bubbles trapped below the water table. Existing NGT models largely attempt to deconvolve the temperature dependent ASW component from the excess air component.

[3] The unfractionated air (UA) model [*Stute and Schlosser*, 1993], which assumes that air bubbles trapped below the water table are quantitatively incorporated into groundwater, thereby adding extra noble gas concentrations in amounts proportional to their partial pressures in the atmosphere, provides the simplest explanation for excess air. The UA model, however, does not always adequately account for measured noble gas concentrations dissolved in groundwater [*Hall et al.*, 2005]. One alternative scheme, the partial re-equilibration (PR) model, which allows for partial loss of the excess air component back to the atmosphere via diffusion of the excess noble gases in water, was subsequently proposed [*Stute et al.*, 1995]. With the development of numerical inversion techniques for converting measured noble gas concentrations into model NGTs [e.g., *Ballentine and Hall*, 1999], it has been possible to apply statistical tests as to whether individual NGT models adequately describe physical processes in the field.

[4] The continuous equilibration (CE) model developed by *Aeschbach-Hertig et al.* [2000] allows for partial absorption of noble gases from air bubbles that are compressed below the water table. The CE model aims to account for apparent relative fractionation of noble gases in the excess air component because the air bubbles are constantly in solubility equilibrium with the surrounding water. One advantage of the CE model is that it correctly predicts that noble gas isotope ratios for groundwater samples should not differ significantly from air values, which contrasts substantially from the PR model [*Peeters et al.*, 2003]. In contrast to the CE and PR models, the negative pressure (NP) model of *Mercury et al.* [2004] explains deviations from the standard UA model via the mechanism of negative pressure within the capillary zone, which modifies noble gas solubilities.

[5] A key assumption common to all of the above models is that the ASW component is the result of equilibration of water with standard air with a relative humidity of nearly 100% and an average pressure determined by the altitude of the recharge zone. Recently, *Hall et al.* [2005] and *Castro et al.* [2007] questioned this core assumption in order to account for a systematic bias of NGTs to values significantly below the average ground temperature. They argued that high measured noble gas concentrations (and hence low NGTs) could be explained by the consumption of O_2 in the unsaturated zone without an equivalent build up of CO_2 (oxygen depletion or OD model of *Hall et al.* [2005]).

[6] In order to test predictions of the OD model, a monitoring water well was drilled in October of 2006, within 30 m of the original domestic well used by *Hall et al.* [2005]. We report new data from this monitoring well

[1]Department of Geological Sciences, University of Michigan, Ann Arbor, Michigan, USA.
[2]Centre de Géosciences, Ecole des Mines de Paris, Fontainebleau, France.

0094-8276/08/2008GL035018$05.00

and develop an alternative NGT model that builds upon the original OD model. This new NGT model better describes noble gas concentrations and remains compatible with measured isotopic ratios.

2. Results and Discussion

[7] The monitoring well has a diameter of 5 cm with a total depth of 24.4 m, extending to the base of the aquifer, with the bottom 12.2 m being screened. The water table has an average depth of 13.3 m and a variation of <0.3 m over the past year. Soil in the unsaturated zone varies from pure sand to clayey sand with some organic matter (Table S1 of the auxiliary material).[1]

[8] Dissolved O_2 (DO) has been measured in the well as a function of water depth using a YSI model 6562 DO sensor attached to a 600XLM sonde. The sensor is calibrated to 100% O_2 saturation using water-saturated air prior to insertion into the well. Measurements were taken continuously as the sonde was slowly lowered into groundwater. A graphical representation of a typical suite of sonde measurements is shown in Figure S1 and DO values for the shallowest measurement sites are given in Table S2, both in the auxiliary material. Shallow DO values range from 20% to 44% of O_2 saturation. In addition, since July 2007, we have been able to monitor CO_2 levels within the screened region above the water table using a Vernier IR CO_2 sensor that can be lowered into the well above the water table. CO_2 levels have ranged from 0.2% to 1.6% (see Table S2), in reasonable agreement with published P_{CO2} values for groundwater in the Huron River drainage area [*Williams et al.*, 2007]. In that study, the mean $\log(P_{CO2})$ value for 22 groundwater samples was −2.13 with a standard deviation of 0.13, corresponding to a mean P_{CO2} of 0.0074 atm., i.e., a concentration of about 0.7%.

[9] DO values at or just above the water table appear to be no more than ~45%, which would be equivalent to an O_2 air content of ~9.5%. Even accounting for a build up of CO_2 in the gas phase due to respiration, the air at the base of the unsaturated zone appears to be missing about 10–11% of its original suite of active gases. This implies that the noble gas pressures at the base of the unsaturated zone must be elevated by a factor of about 1.1, in good agreement with the prediction by *Hall et al.* [2005]. This confirmation of the main prediction of the OD model suggests that some earlier NGT models have possibly calculated the ASW component incorrectly because much of the measured noble gas concentrations have previously been erroneously assigned to the excess air component.

[10] A surprising result from *Hall et al.* [2005] was the presence of significant excess ^3He and ^4He throughout the duration of the study, which suggested a residence time for He of about 30 years, but rapid variations in other chemical parameters (e.g., pH and $\delta^{18}O$ of groundwater) indicated that the water being analyzed had a much shorter mean lifetime. *Hall et al.* [2005] speculated that the groundwater at this site is not in equilibrium with the atmosphere, but instead is buffered by elevated He levels in the unsaturated zone.

[11] On February 11, 2007, a suite of replicate water samples from 8 levels within the well was collected for noble gas analysis. Measured He concentrations are shown in Table S3. Given the known altitude of the site, an average ground temperature of 9.6°C and an overpressure factor of 1.1 from O_2 depletion (P_{OD}), one would expect the He concentration to be 4.94×10^{-8} ccSTP/g, indicating an observed He excess of about 1×10^{-8} ccSTP/g, in good agreement with the excess He values of *Hall et al.* [2005]. With the difference in He concentration at the top of the unsaturated zone (5.3×10^{-6} ccSTP/cc, assuming 100% humidity and a P_{OD} of 1.1) and at the bottom of the unsaturated zone (6.5×10^{-6} ccSTP/cc, assuming equilibrium with average water He concentration at the water table), it is possible to calculate a gradient of 9.0×10^{-10} ccSTP/cc/cm in the gas phase. Assuming steady-state, absence of recharge, constant He flux and similar porosities and tortuosities in the gas and water phases, the expected He concentration gradient in water should just be the above value times the ratio of the diffusion coefficient in gas to that of water. Taking into account the He diffusion coefficient values in water at 9.6°C (5.64×10^{-5} cm^2 s^{-1} [*Jähne et al.*, 1987]) and free air (0.63 cm^2 s^{-1} [*Reid et al.*, 1977]), one would expect a concentration gradient in the water phase of 1.0×10^{-5} ccSTP/g/cm. Accounting for possible effects of vertical mixing during sampling on measured He concentrations, a He concentration gradient in the water phase of $<\sim 1 \times 10^{-11}$ ccSTP/g/cm was estimated (auxiliary material). The predicted gradient, assuming that the gas phase in the unsaturated zone is in equilibrium with groundwater at the water table, is orders of magnitude greater than was measured and thus there appears to be a much lower than predicted flux of He into soil air. Therefore, there is a significant barrier to He transport from the water phase into the gas phase at or near the water table.

[12] The capillary fringe above the water table consists of a region of variable effective gas and water porosity, with low gas content within the pores at the base and high gas content at the top [*van Genuchten*, 1980]. Standard models of gas diffusivity as a function of effective gas porosity [e.g., *Millington and Quirk*, 1961] predict a very strong drop off of effective gas diffusivity as gas porosity declines, a decline caused by a combination of increased tortuosity and decreased connectivity. Field measurements by *Kawamoto et al.* [2006] on soils from Denmark, similar to those found at our field site, revealed that gas diffusion a full meter above the water table can be reduced by more than 3 orders of magnitude below values for free air. Closer to the base of the capillary fringe, effective gas diffusivity can be reduced by 5 orders of magnitude or more. It appears that, at least near the base of the capillary fringe, a region crucial to the formation of the noble gas excess air component, gas diffusion may not always be a particularly fast pathway for equilibration of noble gases. Therefore, slow gas transportation in the capillary fringe may explain the low apparent loss rate of helium into soil air.

[13] The combination of the success of the basic OD model plus evidence for restricted gas diffusion at the base of the unsaturated zones has important implications for existing NGT models. Both the UA and CE models allow for the incorporation of air from disconnected gas-filled pores into groundwater, but once this excess air component is dissolved, it is assumed that there is no re-equilibration with the atmosphere because of the inefficiency of noble gas

[1] Auxiliary materials are available in the HTML. doi:10.1029/2008GL035018.

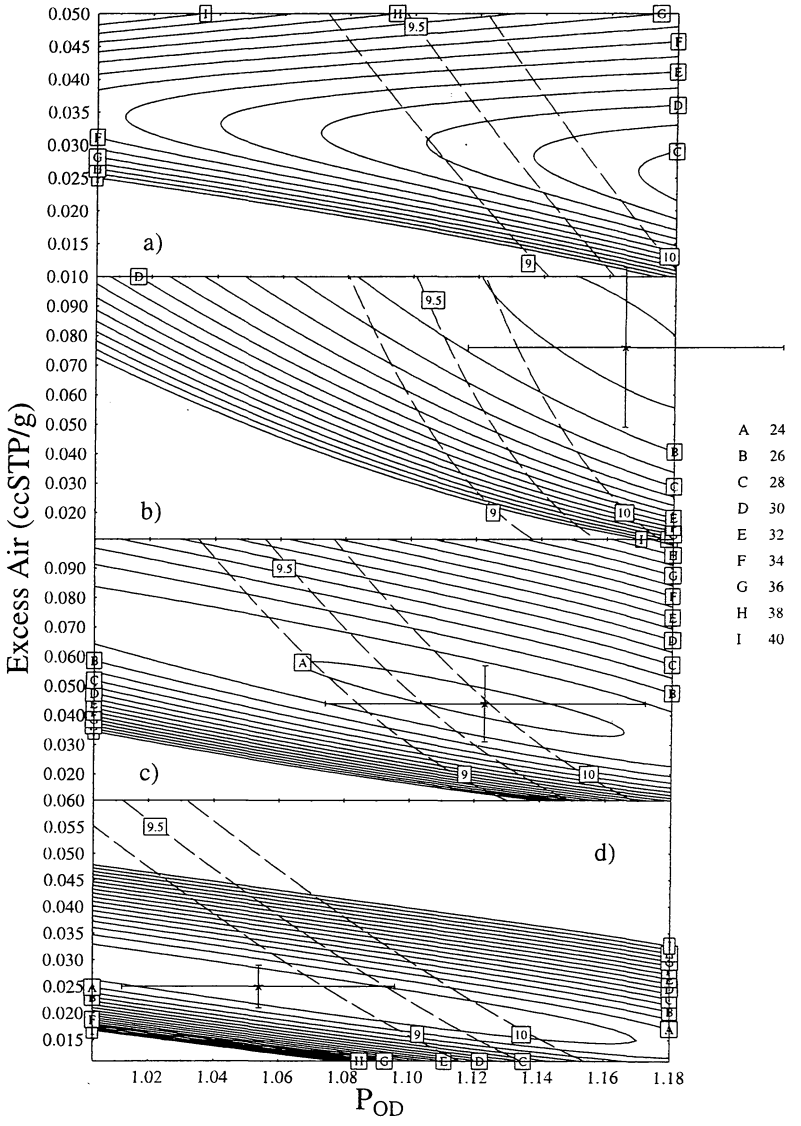

Figure 1. χ^2 goodness of fit surface contours for varying NGT models for *Hall et al.* [2005] data as a function of P_{OD} and excess air (A_e). Contour interval is 1. χ^2 minima error bars estimated from a rise of 1 in the χ^2 value. Also shown are the contours for the average NGT values in dashed lines. Models are: (a) CE model; gas diffusion relaxation models (b) β = 0.5, (c) β = 2/3, and (d) β = 1.

diffusion in water. The PR model does allow for partial re-equilibration, but this is controlled by diffusion in the liquid phase. In all cases, NGT models attempt to account for a frequently large apparent excess of noble gas concentration in measured samples. However, if there is a net deficit of O_2 plus CO_2, this noble gas excess will invariably be over-estimated and therefore much of the effort to provide for fractionated excess air could be biased by the presence of a larger than anticipated ASW component. In addition, if re-equilibration occurs near the water table, at the base of the capillary fringe, the rate limiting process can be diffusion in the gas phase and not necessarily diffusion in water [*Millington and Quirk*, 1961; *Kawamoto et al.*, 2006]. Here we propose a new model to account for measured noble gas concentrations on the basis of the OD model for the ASW component, with allowance for partial re-equilibration of noble gasses between groundwater and soil air via diffusion in the gas phase.

3. Alternative NGT Models

[14] In the original OD model [*Hall et al.*, 2005], excess air was assumed to be unfractionated and was handled in the same manner as the UA model. The overall goodness-of-fit (χ^2) for the entire data set assuming a fixed NGT, although better than that given by the CE model, was still higher than expected (i.e., χ^2 = 343.7 for 69 degrees of freedom). We examine here some alternatives applied to the original *Hall et al.* [2005] data to see if significant improvements might be made.

[15] First, if one takes oxygen depletion into account in the CE model, it is possible to improve that system's performance with this set of data. Figure 1a shows the

result of such an analysis where χ^2 is calculated as a function of the overpressure factor caused by O_2 depletion (P_{OD}) and a single assumed original excess air volume (parameter "A" in the CE model of *Aeschbach-Hertig et al.* [2000]). Their fractionation factor "F" and an NGT value were calculated individually for each of 20 samples, giving 38 degrees of freedom. The minimum χ^2 values within the scanned range of parameters was 27.62 and the probability of a χ^2 variable being greater than or equal to this value is 0.89, indicating that this is an acceptable fit. Also shown in Figure 1a are contours of the average fitted NGT values and although the CE model with the addition of a P_{OD} factor does give an acceptable goodness-of-fit parameter, the minimum value trends to higher NGT values than the actual ground temperature. Nevertheless, the addition of a P_{OD} factor in combination with the CE model does appear to be useful in improving fits and calculating more accurate NGTs.

[16] Next, we examine the possibility that the excess air component, which is not in equilibrium with the soil atmosphere at the water table, will gradually tend to diffuse back into the atmosphere. This is similar to the PR model, but instead of assuming that the diffusion rate of noble gases is determined by the water phase, we examine the possibility of it being dominated by the gas phase. The *Millington and Quirk* [1961] model of dependence of effective diffusion coefficient as a function of porosity is given by:

$$D_e/D_0 = \varepsilon^{10/3}/\phi^2 \quad (1)$$

where D_e is the effective diffusion coefficient, D_0 is the diffusion coefficient in free air, ε is the air filled porosity and ϕ is the total porosity. It is clear that as gas porosity nears zero at the base of the capillary fringe, gas diffusion becomes extremely inefficient [see also *Caron et al.*, 1998; *Kawamoto et al.*, 2006]. The zone just above the water table is likely to be crucial to the formation of the excess air component, as this is where disconnected gas pores are likely to form.

[17] Processes in the boundary layer between air and water will control the transfer of noble gases from water back into the gas phase. *Deacon* [1977] proposed a set of boundary layer models for air-water gas transfer where the mass transfer rate is proportional to D^β, where D is the rate limiting diffusion coefficient, which is often assumed to be the value in water, but at the base of the capillary zone, can be the gas diffusion coefficient. The term β depends on the wind speed over the water, which corresponds here to zero horizontal air speed. In our case of zero horizontal air speed, the preferred value for this parameter was 2/3. Assuming a first order loss of excess air to the gas phase, one can construct a new NGT model, which we will refer to as the gas diffusive relaxation (GR) model, as:

$$C_i = ASW_i \cdot P_{OD} + A_e \cdot Z_i \cdot \exp\left(-\tau \cdot D_i^\beta\right) \quad (2)$$

where C_i is the total concentration of the ith noble gas (i = Ne, Ar, Kr, Xe); ASW_i is the ith air saturated water noble gas component concentration; P_{OD} represents the ratio of noble gas partial pressures at the water table to that in free air (oxygen depletion factor); A_e is the original excess air concentration before interface mass transfer occurs; Z_i represents ith noble gas volume fraction in free air; D_i is the diffusion coefficient of each noble gas in air; β is a mass transfer model dependent constant; and τ is a parameter that depends on the time taken for the gas transfer as well as the length scale of the boundary layer (see the auxiliary material for a derivation of this equation). Gas diffusion coefficients are calculated following *Fuller et al.* [1966].

[18] In practice, we have fixed two of these parameters for the entire suite of data from *Hall et al.* [2005], namely A_e and P_{OD}, and individually fit τ and NGT (which determines ASW_i). The χ^2 statistic for the entire suite of data (38 degrees of freedom) is then calculated for β equal to 0.5, 2/3, and 1 (Figures 1b, 1c, and 1d, respectively). As was the case for the CE model, there are acceptable minima for all three β values (i.e., minimum χ^2 = 24.78, 23.28 and 22.12 with P of χ^2 exceeding these values being 0.95, 0.97 and 0.98 for β = 0.5, 2/3 and 1 respectively). However, the model with $\beta = 2/3$ has a minimum with an average NGT value that closely coincides with the true average temperature of 9.6°C and this is our preferred model. A similar analysis assuming water-based diffusion did not yield acceptable χ^2 values (i.e., $\chi^2 \sim$ degrees of freedom) and tended to have minima that correspond to very high NGT and P_{OD} values.

[19] It should be emphasized that differences between NGT models in their handling of excess air will only be apparent for samples with a significant excess air component (i.e., large excess Ne). The important new feature of the OD and GR models, however, is the recognition of the possibility of soil gas having a noticeably different composition than standard air. This leads to calculating a more accurate ASW component and avoids erroneously ascribing all excess noble gas concentrations to "excess air".

[20] A difficulty with all models that involve noble gas kinetics, where the gases are not in equilibrium, is that such models can predict significant isotope ratio fractionation, as is the case for the PR model. Our new GR model also predicts isotope ratio fractionation, but the effect is small because of two key factors: 1) diffusion coefficients are comparatively insensitive to mass in the *Fuller et al.* [1966] model, being proportional to $(1/M_a + 1/M_i)^{0.5}$, where M_a is the molecular weight of air and M_i is that for the ith noble gas; and 2) the amount of the potentially fractionated component (i.e., excess air) is greatly reduced because of the larger ASW component when $P_{OD} > 1$. Figure 2 shows the predicted and measured $^{40}Ar/^{36}Ar$ ratios for the *Hall et al.* [2005] data using the GR model and the null hypothesis that the two sets of values are not significantly different passes a χ^2 test. The CE model predictions would also satisfy this test.

4. Conclusions

[21] Dissolved oxygen saturation and CO_2 measurements in the new monitoring well support the OD model of *Hall et al.* [2005]. The extremely low measured He concentration gradient within the well suggests that the base of the capillary zone has very low diffusive loss of He, which in turn implies that gas transport from groundwater into the overlying soil gas can be very inefficient. Our new GR model incorporates oxygen depletion and handles the excess air component using a transport model based on boundary

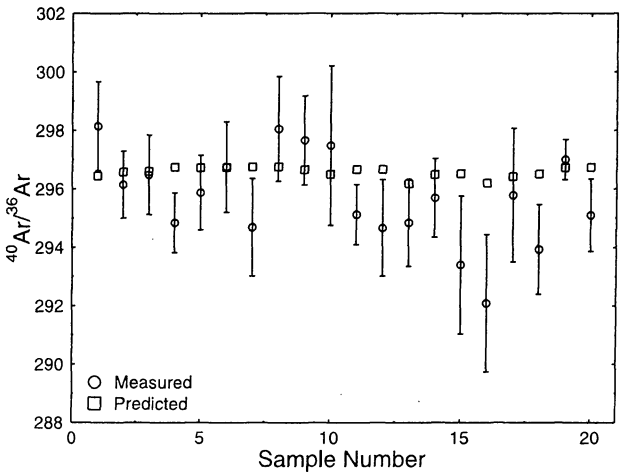

Figure 2. Predicted and measured $^{40}Ar/^{36}Ar$ ratios for *Hall et al.* [2005] data using GR model with $\beta = 2/3$. Errors 1σ. Passes the null hypothesis that the model values and measured ratios are indistinguishable, with $\chi^2 = 22.39$ for 20 degrees of freedom (p = 0.32).

layer gas transfer and is very successful in reproducing the *Hall et al.* [2005] data, including isotopic ratios. Applying an oxygen depletion correction also improves the ability of the CE model to reproduce the data. The GR model assumes unfractionated excess air incorporation, but partial re-equilibration, while the CE model has fractionated excess air uptake with no re-equilibration. It is possible that either mechanism, or a combination of both, is operating at any given site. Further characterization of both groundwater and soil gas compositions will be required to test our new hypothesis, both at this site as well as other locations spanning a range of climates.

[22] **Acknowledgments.** The authors thank two anonymous reviewers for their constructive reviews. Financial support by the National Science Foundation CAREER award EAR 0545071 is greatly appreciated.

References

Aeschbach-Hertig, W., F. Peeters, U. Beyerle, and R. Kipfer (2000), Paleotemperature reconstruction from noble gases in ground water taking into account equilibration with entrapped air, *Nature*, *405*, 1040–1044.

Ballentine, C. J., and C. M. Hall (1999), Determining paleotemperature and other variables by using an error-weighted nonlinear inversion of noble gas concentrations in water, *Geochim. Cosmochim. Acta*, *63*, 2315–2336.

Caron, F., G. Manni, and W. J. G. Workman (1998), A large-scale laboratory experiment to determine the mass transfer of CO_2 from a sandy soil to moving groundwater, *J. Geochem. Explor.*, *64*(1–3), 111–125, doi:10.1016/S0375-6742(98)00024-7.

Castro, M. C., C. M. Hall, D. Patriarche, P. Goblet, and B. R. Ellis (2007), A new noble gas paleoclimate record in Texas—Basic assumptions revisited, *Earth Planet. Sci. Lett.*, *257*(1–2), 170–187, doi:10.1016/j.epsl.2007.02.030.

Deacon, E. L. (1977), Gas transfer to and across an air-water-interface, *Tellus*, *29*(4), 363–374.

Fuller, E., P. Schettler, and J. Giddings (1966), A new method for prediction of binary gas-phase diffusion coefficients, *Ind. Eng. Chem.*, *58*(5), 19–27.

Hall, C. M., M. C. Castro, K. C. Lohmann, and L. Ma (2005), Noble gases and stable isotopes in a shallow aquifer in southern Michigan: Implications for noble gas paleotemperature reconstructions for cool climates, *Geophys. Res. Lett.*, *32*, L18404, doi:10.1029/2005GL023582.

Heaton, T. H. E., and J. C. Vogel (1981), "Excess air" in groundwater, *J. Hydrol.*, *50*(1–4), 201–216.

Jähne, B., G. Heinz, and W. Dietrich (1987), Measurement of the diffusion coefficients of sparingly soluble gases in water, *J. Geophys. Res.*, *92*, 10,767–10,776.

Kawamoto, K., P. Moldrup, P. Schjønning, B. V. Iversen, D. E. Rolston, and T. Komatsu (2006), Gas transport parameters in the vadose zone: Gas diffusivity in field and lysimeter soil profiles, *Vadose Zone J.*, *5*(4), 1194–1204, doi:10.2136/vzj2006.0014.

Mercury, L., D. L. Pinti, and H. Zeyen (2004), The effect of the negative pressure of capillary water on atmospheric noble gas solubility in ground water and paleotemperature reconstruction, *Earth Planet. Sci. Lett.*, *223*(1–2), 147–161, doi:10.1016/j.epsl.2004.04.019.

Millington, R. J., and J. P. Quirk (1961), Permeability of porous solids, *Trans. Faraday Soc.*, *57*, 1200–1207.

Peeters, F., U. Beyerle, W. Aeschbach-Hertig, J. Holcher, M. Brennwald, and R. Kipfer (2003), Improving noble gas based paleoclimate reconstruction and groundwater dating using $^{20}Ne/^{22}Ne$ ratios, *Geochim. Cosmochim. Acta*, *67*(4), 587–600.

Reid, R. C., J. M. Prausnitz, and T. K. Sherwood (1977), *The Properties of Gases and Liquids*, 3rd ed., McGraw-Hill, New York.

Stute, M., and P. Schlosser (1993), Principles and applications of the noble gas paleothermometer, in *Climate Change in Continental Isotopic Records*, *Geophys. Monogr. Ser.*, vol. 78, edited by P. K. Swart et al., pp. 89–100, AGU, Washington, D. C.

Stute, M., M. Forster, H. Frischkorn, A. Serjo, J. F. Clark, P. Schlosser, W. S. Broeker, and G. Bonani (1995), Cooling of tropical Brazil (5°C) during the last glacial maximum, *Science*, *269*, 379–383.

van Genuchten, M. T. (1980), A closed-form equation for predicting the hydraulic conductivity of unsaturated soils, *Soil Sci. Soc. Am. J.*, *44*, 892–898.

Williams, E. L., K. J. Szramek, L. Jin, T. C. W. Ku, and L. M. Walter (2007), The carbonate system geochemistry of shallow groundwater–surface water systems in temperate glaciated watersheds (Michigan, USA): Significance of open-system dolomite weathering, *Geol. Soc. Am. Bull.*, *119*(5–6), 515–528, doi:10.1130/B25967.1.

M. C. Castro, C. M. Hall, K. C. Lohmann, and T. Sun, Department of Geological Sciences, University of Michigan, 2534 C. C. Little Building, Ann Arbor, MI 48109-1005, USA. (welsumm@umich.edu)

P. Goblet, Centre de Géosciences, Ecole des Mines de Paris, 35, Rue Saint-Honoré, F-77305 Fontainebleau, France.

Auxiliary Material for Paper 2008GL035018

Tie Sun Chris M. Hall Maria Clara Castro
Kyger C. Lohmann Patrick Goblet

1 Soil Characteristics

Descriptions of the soil and sub-soil layers deduced from core samples retrieved and sediment discharge during the drilling of the monitoring well are given in Table A1.

2 CO_2 And Dissolved O_2 (DO) Measurements

Measurements of CO_2 concentration for some of the sampling dates are given in Table A2. There was significant variation between sampling days and there was a general trend for CO_2 concentration to decrease as the sensor was lowered toward the water table.

Groundwater parameters that were monitored using the YSI sonde were measured *in situ* and did not involve significant mixing within the well. Figure A1 shows the results from a traverse down the well taken on Oct. 7, 2007 and it illustrates the typical kind of data that the sonde provides . From the fine detail that can be seen in these records, it is clear that there is very little vertical mixing caused by the movement of the sonde down the well. Dissolved oxygen (DO) invariably declines as the sonde is lowered below the water table. DO values from the shallowest sonde positions for a suite of measurement dates are shown in Table A2 and these place a lower limit on the oxygen saturation immediately above the water table.

3 Sampling Procedure And Interpretation Of Helium Data

On February 11, 2007, a series of samples were collected from eight distinct depths within the well (Table A3). Samples were collected sequentially from the top part of aquifer to the bottom. The first two samples (1a and 1b)

were collected 0.12 m below the water table, and the second two samples (2a and 2b) were collected 0.57 m below the water table, and so on (Table A3). The average pumping rate from the Proactive model P- 10330 12V DC pump used was $\sim$ 4 l/min (0.07 l/s). The total time spent pumping at each location for both samples was $\sim$ 10 minutes. The goal of such methodical, sequential sampling was to minimize the vertical mixture effect within the well. However, due to the requirement to withdraw water for several minutes to obtain high quality samples, there was still significant mixing of water from different levels while sampling at each location. What follows is an analysis that attempts to estimate the effects of vertical mixing and that allow us to place reasonable limits on the actual helium concentration gradient based upon our measurements.

Upward vertical water flow into the well from below can be neglected due to the presence of a massive clay layer at the bottom of the well. Under these conditions, and assuming a constant hydraulic conductivity in the well, it is possible to make a simplified estimate of both water flow toward the well and vertical flow within the well. Let the vertical position within the well be given by z where the bottom of the well is at $z = 0$ and the water table is at $z = H$ (Fig A2). Three reasonable assumptions (approximations) are made: a) the hydraulic conductivity within the well pipe is much greater than within the saturated zone; b) the drop in hydraulic head is constant throughout the entire water column within the well, and; c) the hydraulic conductivity is nearly constant within the saturated zone near the well (see, e.g., Table A1). Under these conditions, flow toward the well will be purely horizontal and constant along the entire depth of the aquifer, while the vertical flow rate within the pipe will be linearly dependent on the distance from the pump intake, with zero vertical flow at both the top and the bottom of the aquifer. Given a total pumping rate of Q and a pump location below the water table of p, the vertical flow rate can be written as:

$$\begin{aligned} q(z) &= \frac{-Q}{H}(H - z) \quad z > H - p \\ &= \frac{Qz}{H} \qquad\quad z < H - p \end{aligned} \tag{1}$$

where flow downward is negative. The flow rate in the immediate vicinity of the pump is proportional to the distance to the boundaries, i.e. Qp/H above, and $Q(H - p)/H$ below.

Vertical flow velocity $V(z)$ is given by the flow rate divided by the cross sectional area of the pipe (S) as follows:

$$\begin{aligned} V(z) &= \frac{-Q}{HS}(H - z) \quad z > H - p \\ &= \frac{Qz}{HS} \qquad\quad z < H - p \end{aligned} \tag{2}$$

The time $t(z)$ needed for water within the pipe starting at z to arrive in the vicinity of the pump's intake will be given by the integral of the reciprocal of the vertical velocity, i.e.:

$$t(z) = \int_z^{H-p} \frac{dx}{V(x)} \tag{3}$$

From equations 2 and 3:

$$\begin{array}{rcll} t(z) & = & \int_z^{H-p} \frac{-HS}{Q(H-x)} dx & = \frac{HS}{Q} \ln\left(\frac{p}{H-z}\right) \quad z > H-p \\ & = & \int_z^{H-p} \frac{HS}{Qx} dx & = \frac{HS}{Q} \ln\left(\frac{H-p}{z}\right) \quad z < H-p \end{array} \tag{4}$$

The maximal sampling extent for a given pumping time τ is given by the distance traveled by water in the well that just reaches the pump inlet at the end of the pumping duration. Let us denote the maximum sampling location above the pump as z_a and the lowest sampled location below the pump as z_b. From equation 4 we can write:

$$\begin{array}{rcll} z_a & = & H - pe^{-Q\tau/HS} & z > H-p \\ z_b & = & (H-p)e^{-Q\tau/HS} & z < H-p \end{array} \tag{5}$$

For pumping time τ, the amount of sample from a given level z is proportional to the time it spends in the vicinity of the pump intake. A distribution function $f(z)$ gives the contribution of water from each level within the aquifer. Since water cannot reach the pump if $z > za$ or if $z < zb$, for those parts of the aquifer $f(z) = 0$. Let $f(z)$ be the time a parcel of water is near the pump intake:

$$\begin{array}{rcll} f(z) & = & \tau - \frac{HS}{Q} \ln\left(\frac{p}{H-z}\right) & z > H-p \\ & = & \tau - \frac{HS}{Q} \ln\left(\frac{H-p}{z}\right) & z < H-p \end{array} \tag{6}$$

The maximum contribution is thus from $z = p$ where $f(z) = \tau$.

Let the He concentration at level z be $C(z)$ and the measured concentration, which will be a weighted average of water from z_a to z_b, be C_{meas}. The measured concentration should then be given by:

$$C_{meas} = \frac{\int_{z_a}^{z_b} C(x)f(x)dx}{\int_{z_a}^{z_b} f(x)dx} \tag{7}$$

Assuming steady-state, with constant helium flux, $C(z)$ will be a linear function of the vertical position within the aquifer, so we can write:

$$C(z) = a + bz \tag{8}$$

Combining equations 7 and 8 gives:

$$C_{meas} = a + b\frac{\int_{z_b}^{z_a} x f(x)dx}{\int_{z_b}^{z_a} f(x)dx} = a + bz_m \tag{9}$$

where z_m is the effective mid-point of the weighted average that is sampled at depth p when the pump is run for a period of time τ. The effective pump sampling depth is $p_m = H - z_m$.

The parameters for the 16 samples taken for the vertical traverse of the aquifer are given in Table A3. It is clear that there is a shift of the effective mean sampling depth (p_m) from the pump position (p), but in all cases the difference is less than 3.2m and in most cases, the difference is much less than 2m. Although the effective depth range that was sampled is less than the range in pump depths, there is still a sufficient distance covered (> 6m) to be able to detect the presence of a significant He concentration gradient.

In order to place error limits on the vertical He concentration gradient at the site, we have fit the data in Table A3 (i.e. He vs. p_m) to a straight line using the algorithm of York (1969) while assuming an error of 1.5% in concentration (Hall et al., 2005) and an error of 1m in depth. The resulting fit gives a gradient of -6.6x10$^{-13}\pm$ 1.1x10^{-11} (2σ) ccSTP/g/cm with mean squared weighted deviates (MSWD) of 1.54, indicating that we expect the actual He gradient to be less than $\sim$ 1x10^{-11} ccSTP/g/cm (Fig. A3). This is within error of being a zero apparent vertical He concentration gradient and indicates that there is an extremely low vertical He flux within the saturated zone.

4 Oxygen Depletion (OD) Model Equation

Oxygen and CO_2 account for $\sim$ 20% of the volume fraction in the dry atmosphere (Ozima and Podosek 1983). However, in the unsaturated zone, oxygen is converted into water and CO_2 by organic matter and bacteria. As noted by Hall et al. (2005), the high solubility of CO_2 compared to oxygen makes it likely that the depletion of O_2 in the gas phase will not be matched by an equal build up of CO_2. Instead, much of the CO_2 production will quickly enter the liquid phase within the unsaturated zone and at the water table. Thus, at the bottom of the unsaturated zone, just above the water table, the total volume fraction of oxygen plus CO_2 is likely to be significantly depressed relative to their values in free air. The low (< 50%) measured dissolved O_2 saturation within groundwater plus the measured

CO_2 concentration within the gas phase just above the water table as documented within the manuscript strongly supports the likelihood of a depleted O_2 zone at the water table.

For example, if half of the oxygen is converted into H_2O and CO_2 in the unsaturated zone and if there is only 1% CO_2 in the gas phase, then the total of O_2 and CO_2 will only constitute about 11% of the air at the base of the unsaturated zone. The remaining gases such as N_2 and the noble gases will have their partial pressures increased to maintain total atmospheric pressure and the net effect will be to have all noble gas partial pressures increased by a factor of about 1.1.

Let the ratio of noble gas partial pressure above the water table to that in the free atmosphere be P_{OD}. The ASW component at the water table for the ith noble gas will thus be the standard value ASW_i times the P_{OD} factor. When unfractionated excess air is added, then noble gas concentrations in groundwater can be calculated as:

$$C_i = ASW_i \cdot P_{OD} + A_e \cdot Z_i \tag{10}$$

where C_i is the total concentration of the ith noble gas (i = Ne, Ar, Kr, Xe); ASW_i is the standard ith air saturated water noble gas component concentration; P_{OD} represents the ratio of noble gas partial pressures at the water table to that in free air (oxygen depletion factor); A_e is the excess air concentration; Z_i represents ith noble gas volume fraction in free air.

5 GR Model Derivation

Assuming standard atmospheric pressure, the air saturated water component of the ith noble gas in quiescent water is denoted by ASW_i. Then, under increased partial pressure P_{OD}, the ith ASW component equals $ASW_i \cdot P_{OD}$. After excess air A_e is totally dissolved, the ith noble gas ASW concentration is $ASW_i \cdot P_{OD} + C_{excess,0i}$ where $C_{excess,0i}$ equals $A_e \cdot Z_i$. Consequently, total concentration of ith noble gas in groundwater equals $ASW_i \cdot P_{OD} + A_e \cdot Z_i$.

Because excess air is dissolved, the noble gas in groundwater is out of equilibrium with the gas in the soil air and noble gases in the groundwater will tend to diffuse back to the soil air. This interface flux of noble gas diffusing back to soil air can be described by the boundary layer model of Deacon et al. (1977), which suggests that interface gas exchange rate between water and air is proportional to the excess gas concentration ($C_{excess,i}$) and is also

proportional to D_i^β, where D_i is the diffusivity of the ith gas in the rate-limiting phase and β is a parameter depending on the wind speed over the gas exchange interface. Thus, we have:

$$J_i = C_{excess,i} \cdot \alpha \cdot D_i^\beta \tag{11}$$

where J_i is air-water interface flux rate; α is a constant determined by interface properties; and D_i is the ith gas diffusion coefficient in the rate-limiting phase. Given that the flux can be described as the rate of change of the excess noble gas concentration, we have:

$$J_i = -\frac{dC_{excess,i}}{dt} \tag{12}$$

Combining equation 11 and 12, we get $\frac{dC_{excess,i}}{dt} = -C_{excess,i} \cdot \alpha \cdot D_i^\beta$ and thus,

$$C_{excess,i} = \exp(-\alpha \cdot D_i^\beta \cdot t) \cdot C_{excess,i0} \tag{13}$$

where $C_{excess,i0}$ is the initial excess gas concentration (i.e., $A_e Z_i$). Therefore, $C_{excess,i} = \exp(-\alpha \cdot D_i^\beta \cdot t) \cdot A_e \cdot Z_i$ and by setting $\tau = \alpha \cdot t$, we get

$$C_{excess,i} = A_e \cdot Z_i \cdot \exp(-\tau \cdot D_i^\beta) \tag{14}$$

Therefore, the total ith noble gas concentration predicted by the GR model in groundwater is

$$C_i = P_{OD} \cdot ASW_i + A_e \cdot Z_i \cdot \exp(-\tau \cdot D_i^\beta) \tag{15}$$

By applying the mass dependent diffusion coefficient for different isotopes, it is possible to predict what the isotopic composition of any noble gas would be for given values of A_e and τ. We show the results of this calculation for $^{40}Ar/^{36}Ar$ ratios for the Hall et al. (2005) samples in Table A4.

6 Chi-Squared Analysis

Figure 1 (main text) shows the results of fitting NGT models to the full suite of noble gas measurements from the Hall et al. (2005) study. There were 20 samples analyzed in that study and for each there was a Ne, Ar, Kr and Xe concentration determined for the purposes of NGT estimation. Therefore, there are a total of 80 concentration measurements. For any given NGT model, a set of input parameters can be used to estimate model

noble gas concentrations M_i, where i = Ne, Ar, Kr and Xe. If the measured values are C_i with estimated errors σ_i, then the error-weighted misfit for each measurement can be written as

$$s_i = \left(\frac{M_i - C_i}{\sigma_i}\right)^2 \tag{16}$$

The total error-weighted misfit S for the entire suite of samples, can be written as:

$$S = \sum_j \sum_i s_{ij} \tag{17}$$

where $1 \leq j \leq 20$. For all models, A_e and P_{OD} were set to a single value for the entire suite of measurements and their best values were estimated by finding the minimum for S. For the CE model, individual values of F and T were estimated, while for the GR model, individual values of τ and T were fitted. S should be a χ^2 statistic with 38 degrees of freedom as there are 80 measurements with $20 \times 2 + 2 = 42$ fitted parameters. The results of the analysis are shown in Figure 1 (main text).

References

[1] Deacon, E. L. (1977), Gas transfer to and across an air-water-interface. *Tellus, 29*, 363- 374.

[2] Hall, C. M., M. C. Castro, K. C. Lohmann, and L. Ma (2005), Noble gases and stable isotopes in a shallow aquifer in southern Michigan: Implications for noble gas paleotemperature reconstructions for cool climates, *Geophys. Res. Lett., 32*, L18404, doi:10.1029/2005GL023582.

[3] Ozima, M. and Podosek, F.A . (1983) *Noble gas geochemistry.* Cambridge Univ. Press, Cambridge, U.K., 377pp.

[4] York, D. (1969), Least squares fitting of a straight line with correlated errors. *Earth Planet. Sci. Lett., 5*, 320-324.

7 Figure Captions

7.1 Figure A1

File 2008gl035018-fa1.eps. Sonde data collected on Oct. 7, 2007. Shown are dissolved oxygen (DO) in percent saturation, *in situ* temperature (°C), pH, salinity in parts per thousand (ppt) and oxygen redox potential (mV) as a function of depth below the water table (m). Multiple readings were taken at each depth location as the sonde was slowly lowered into the well. The sonde was left at a site until the sensors settled to a constant value.

7.2 Figure A2

File 2008gl035018-fa2.eps. Cartoon showing the monitoring well. Vertical extent is from $z = 0$ to $z = H$ and pump intake is at $z = H - p$.

7.3 Figure A3

File 2008gl035018-fa3.eps. Helium concentration as a function of p_m, the effective sampling midpoint as defined in the text of the auxiliary material. Shown are the best linear fit along with the maximum helium gradient ($+2\sigma$) supported by the measured values. Maximum slope line is fit through the centroid of the data (York, 1969).

Layer #	Core Description	Depth of Layer Bottom (m)	Layer Thickness (m)
1	surface soil, brown fine sand with tree root	0.19	0.19
2	gravel	2.07	1.88
3	gravel with fine sand	3.22	1.15
4	gravel	3.71	0.49
5	sand	5.08	1.37
6	fine sand	6.40	1.32
7	gravel	8.07	1.67
8	sand	13.43	5.36
9	powdery sand with rock fragments and some organic matter	14.04	0.61
10	sand	17.09	3.05

Table 1: (A1) Soil descriptions based on cores retrieved during drilling of the monitoring well.

Date	Depth of Sonde Sensors Below Water Table (m)	Dissolved O_2 (%)	CO_2 Concentration Above Water Table (%)
04/21/07	0.519	20.0	
05/19/07	0.105	34.8	
06/02/07	0.014	40.7	
06/09/07	0.013	33.5	
06/16/07	0.005	40.7	
07/14/07	0.199	40.1	1.56
08/04/07	0.006	25.6	0.89
08/18/07	0.140	27.7	0.30
09/01/07	0.007	28.7	0.49
10/07/07	0.010	43.7	0.16

Table 2: (A2) Dissolved oxygen values in shallowest groundwater measurements as a function of time during the study. Also shown are CO_2 values in air just above the water table for sampling dates since 7/14/07.

Sample	T (°C)	He ccSTP/g $\times 10^8$	Pump Depth p (m)	Pump Rate Q ($m^3 s^{-1}$)	z_a (m)	z_b (m)	z_m (m)	Sampling Midpoint p_m (m)
1a	8.6	6.07	0.12	6.3E-05	11.24	5.53	9.21	2.09
1b	8.6	5.96	0.12	6.3E-05	11.27	2.62	8.01	3.29
2a	8.7	6.21	0.57	6.3E-05	11.02	5.31	8.92	2.38
2b	8.7	6.14	0.57	6.3E-05	11.16	2.62	7.87	3.43
3a	8.8	5.86	1.03	6.3E-05	10.79	5.08	8.62	2.68
3b	8.8	5.92	1.03	6.3E-05	11.05	2.51	7.67	3.63
4a	8.6	6.03	2.86	6.3E-05	9.89	4.17	7.44	3.86
4b	8.6	5.96	2.86	6.3E-05	10.60	2.06	6.87	4.43
5a	8.6	5.79	4.69	5.1E-05	8.64	3.74	6.32	4.98
5b	8.6	6.26	4.69	5.1E-05	9.80	2.11	6.13	5.17
6a	8.7	6.17	6.52	2.1E-05	6.14	3.78	4.90	6.40
6b	8.7	6.20	6.52	2.1E-05	7.22	2.99	5.01	6.29
7a	8.8	6.04	8.35	7.6E-05	7.73	1.26	4.05	7.25
7b	8.7	5.95	8.35	7.6E-05	9.77	0.54	4.63	6.67
8a	8.8	5.92	10.17	7.6E-05	6.95	0.48	2.98	8.32
8b	8.8	5.97	10.17	7.6E-05	9.44	0.21	3.94	7.36

Table 3: (A3) He concentration profile within the well. In addition to pump depth and pump rate, we also show the estimated effective mean sampling depth (p_m) as described in the auxiliary material text. For "a "samples, τ=300s, for "b" samples τ=600s. H = 11.3m and S = 2.376e-3m^2. Estimated 1σ uncertainties in concentration are 1.5%. Temperatures were measured at the outflow from the sampling tube.

Sample	Measured $^{40}Ar/^{36}Ar$	Error	Predicted $^{40}Ar/^{36}Ar$	$\%Ar_{exc}$
1A	298.1	1.5	296.4	8.3
2A	296.1	1.1	296.6	10.2
2B	296.5	1.4	296.6	10.9
3A	294.8	1.0	296.7	14.4
3B	295.9	1.3	296.7	12.7
4A	296.8	1.6	296.7	14.6
4B	294.7	1.7	296.7	14.0
5A	298.0	1.8	296.8	14.3
5B	297.7	1.5	296.7	12.4
6B	297.5	2.7	296.5	9.1
7A	295.1	1.0	296.7	12.4
7B	294.7	1.7	296.7	11.9
8A	294.8	1.5	296.2	4.9
8B	295.7	1.3	296.5	9.0
9A	293.4	2.4	296.5	9.6
9B	292.1	2.4	296.2	5.1
10A	295.8	2.3	296.4	8.0
10B	293.9	1.5	296.5	9.2
11A	297.0	0.7	296.7	14.5
11B	295.1	1.2	296.7	14.2

Table 4: (A4) Measured and predicted $^{40}Ar/^{36}Ar$ ratios for the data from Hall et al. (2005) using the GR model (see manuscript and auxiliary material text). Errors are 1σ. The total χ^2 statistic for the suite of samples is 22.4 with 20 degrees of freedom indicating that the null hypothesis that the measurements are not distinguishable from the model passes. Ar_{exc} is the amount of Ar in the excess air component.

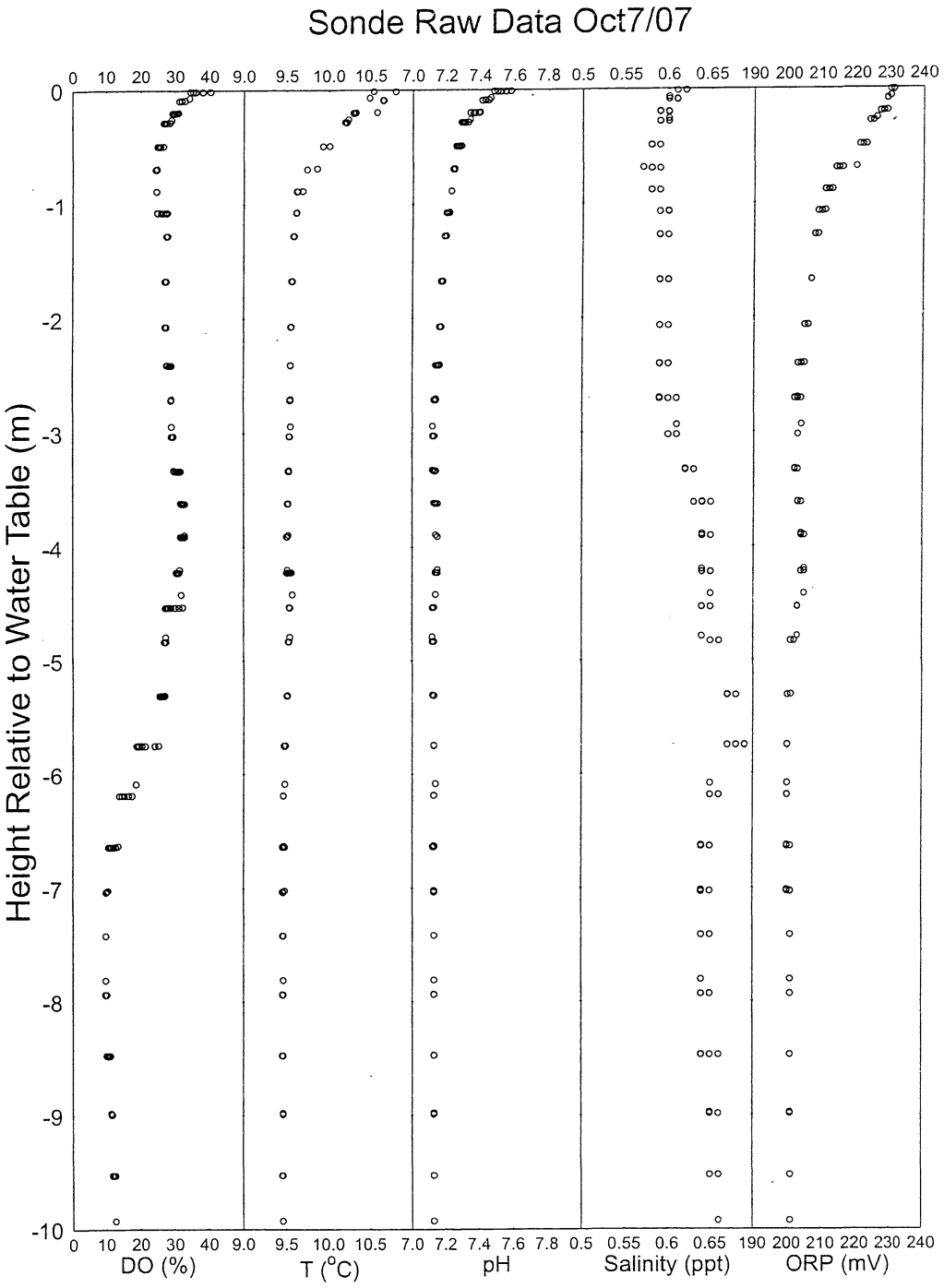
Sonde Raw Data Oct7/07
Height Relative to Water Table (m)
0
-1
-2
-3
-4
-5
-6
-7
-8
-9
-10
0 10 20 30 40
DO (%)
9.0 9.5 10.0 10.5
T (°C)
7.0 7.2 7.4 7.6 7.8
pH
0.5 0.55 0.6 0.65
Salinity (ppt)
190 200 210 220 230 240
ORP (mV)

Fig. A1

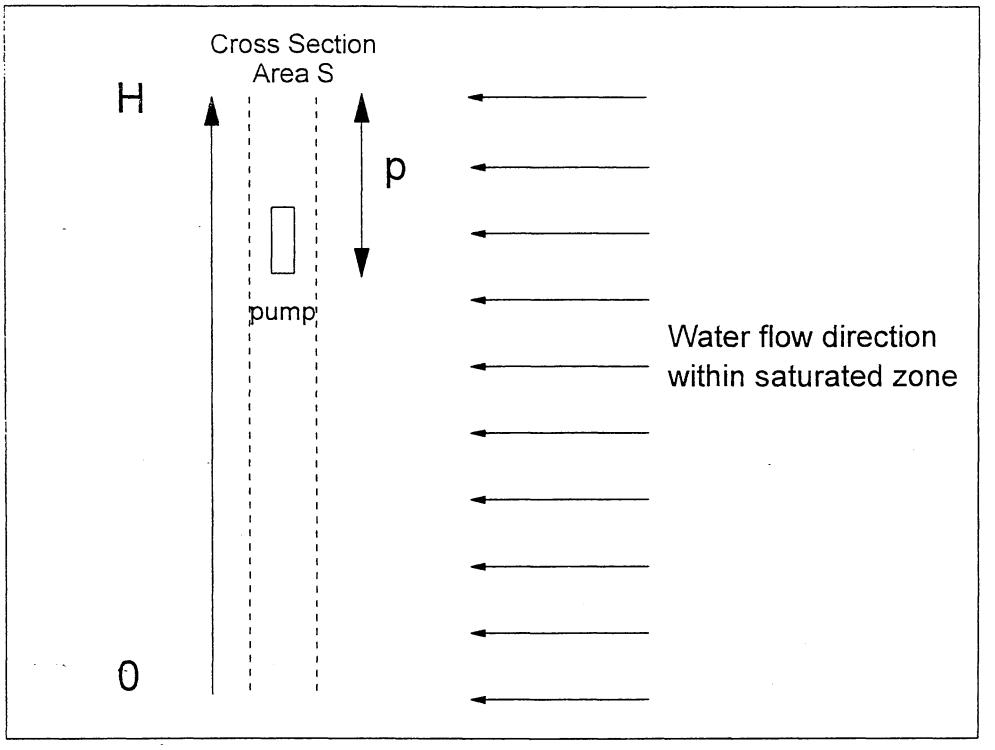
Cross Section
Area S
H
p
pump
Water flow direction
within saturated zone
0

Fig. A2

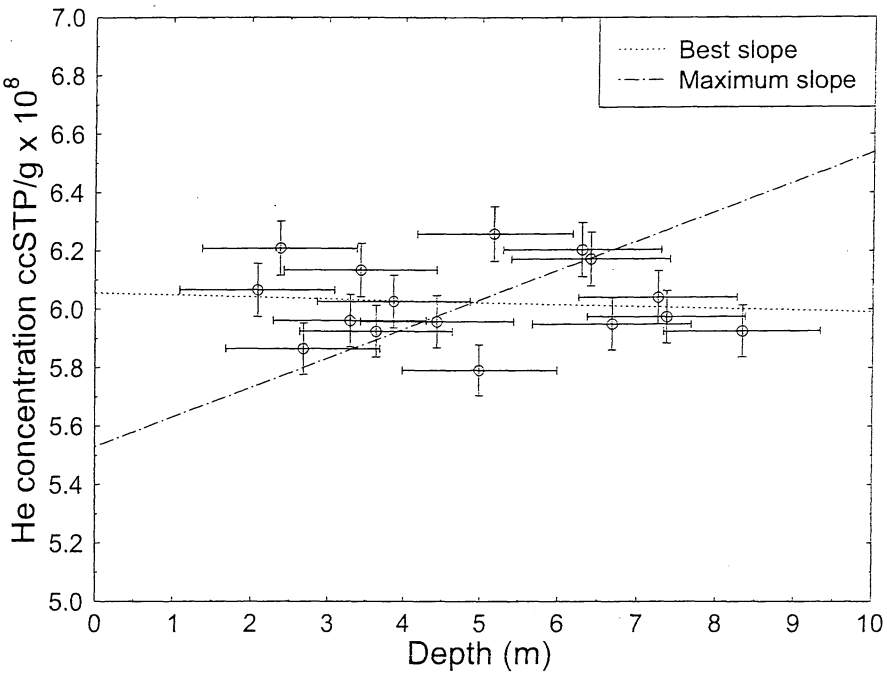
Best slope
Maximum slope
He concentration ccSTP/g x 10^8
Depth (m)
7.0
6.8
6.6
6.4
6.2
6.0
5.8
5.6
5.4
5.2
5.0
0
1
2
3
4
5
6
7
8
9
10

Fig. A3